The temperature dependence of the local tunnelling conductance in cuprate superconductors with competing AF order

Hong-Yi Chen and C.S. Ting
Texas Center for Superconductivity and Advanced Material, and Department of Physics, University of Houston, Houston, TX 77204

Based on the $t-t'-U-V$ model with proper chosen parameters for describing the cuprate superconductors, it is found that near the optimal doping at low temperature (T), only the pure d-wave superconductivity (dSC) prevails and the antiferromagnetic (AF) order is completely suppressed. At higher T, the AF order with stripe modulation and the accompanying charge order may emerge, and they could exist above the dSC transition temperature. We calculate the local differential tunnelling conductance (LDTC) from the local density of states (LDOS) and show that their energy variations are rather different from each other as T increases. Although the calculated modulation periodicity in the LDTC/LDOS and bias energy dependence of the Fourier amplitude of LDTC in the "pseudogap" region are in good agreement with the recent STM experiment [Vershinin *et al.*, Science **303**, 1995 (2004)], we point out that some of the energy dependent features in the LDTC do not represent the intrinsic characteristics of the sample.

PACS numbers: 74.25.Jb, 74.20.-z, 74.50.+r

Recently, STM or the local differential tunnelling conductance (LDTC) measurement by Vershinin *et al.* [1] on slightly underdoped BSCCO indicated that the electronic states at low energies and at a temperature T higher than the superconducting transition temperature (T_c) in the pseudogap region exhibit an energy-independent spatial modulation which resulting to a checkerboard pattern with incommensurate periodicity $4.7a \pm 0.2$ (a is the lattice constant). At very low temperature, however, no such pattern has been detected [1], in agreement with previous measurements [2, 3]. In addition, the Fourier amplitude of the LDTC at the modulation wave-vector which corresponds the periodicity $4.7a$ increases its magnitude first and then flattens out as the bias energy decreases. How to understand these behaviors are outstanding questions which have not been addressed in the existing literatures. In the present paper we are trying to explain these issues by adopting the idea of the possible coexistence of the d-wave superconductivity (dSC) with antiferromagnetic (AF) order for cuprate superconductors [4, 5, 6, 7], and to examine the formation of the AF order and the accompanying charge order at finite temperature. The phenomenological $t-t'-U-V$ model will be applied to describe the cuprate superconductors. With proper chosen parameters, we show that at low temperature only dSC prevails in our system and the AF order is completely suppressed. The local density of states (LDOS) and LDTC images are featureless. At higher temperature, it is found that the AF order with stripe modulation, which is also referred to the spin density wave (SDW), and the accompanying charge order or the charge density wave (CDW) may show up and they could even persist at temperatures above the BCS superconducting transition temperature T_c^{BCS}. In the presence of SDW, we show both of the LDOS/LDTC images to have energy-independent stripe modulation with spacing of $5a/4a$ spreading over a $48a \times 24a$ lattice. According to the Fourier analysis of the LDOS images, an average periodicity $4.8a$ could be assigned for the stripe modulation. If both of the doubly degenerate x- and y- oriented stripes have the probability to appear in the time interval of the measurement or the proximity effect [8] exists between neighboring domains with differently oriented stripe modulations, the combined LDOS images would have a checkerboard pattern of $4.8a \times 4.8a$ structure. All these features are consistent with the experiment of Vershinin *et al.* [1]. In order to compare with the energy variation of the STM measurements at finite temperature (T), the LDTC is needed and it can be obtained from the LDOS by using the method of convolution. although both of the energy variations of LDTC and LDOS exhibit the "pseudogap"-like characteristics [9], their behaviors at higher temperature are quite different. While the size of the gap for quasiparticle excitations as a function of T is measured by the separation between the coherent peaks in the LDOS, the use of the LDTC or the experimental data to directly determined this quantity could be misleading.

To model these observed phenomena, we employ an effective mean-field $t-t'-U-V$ Hamiltonian by assuming that the on-site repulsion U is responsible for the competing antiferromagnetism and the nearest-neighbor attraction V causes the d-wave superconducting pairing

$$\begin{aligned} \mathbf{H} &= -\sum_{\mathbf{ij}\sigma} t_{\mathbf{ij}} c^{\dagger}_{\mathbf{i}\sigma} c_{\mathbf{j}\sigma} + \sum_{\mathbf{i}\sigma} (U\langle n_{\mathbf{i}\bar{\sigma}}\rangle - \mu) c^{\dagger}_{\mathbf{i}\sigma} c_{\mathbf{i}\sigma} \\ &\quad + \sum_{\mathbf{ij}} (\Delta_{\mathbf{ij}} c^{\dagger}_{\mathbf{i}\uparrow} c^{\dagger}_{\mathbf{j}\downarrow} + \Delta^{*}_{\mathbf{ij}} c_{\mathbf{j}\downarrow} c_{\mathbf{i}\uparrow}) \,, \end{aligned} \tag{1}$$

where $t_{\mathbf{ij}}$ is the hopping integral, μ is the chemical potential, and $\Delta_{\mathbf{ij}} = \frac{V}{2}\langle c_{\mathbf{i}\uparrow} c_{\mathbf{j}\downarrow} - c_{\mathbf{i}\downarrow} c_{\mathbf{j}\uparrow}\rangle$ is the spin-singlet d-wave bond order parameter. The Hamiltonian above

shall be diagonalized by using Bogoliubov-de Gennes' (BdG) equations,

$$\sum_{\mathbf{j}}^{N} \begin{pmatrix} \mathcal{H}_{ij\sigma} & \Delta_{\mathbf{ij}} \\ \Delta^*_{\mathbf{ij}} & -\mathcal{H}^*_{\mathbf{ij}\bar{\sigma}} \end{pmatrix} \begin{pmatrix} u^n_{\mathbf{j}\sigma} \\ v^n_{\mathbf{j}\bar{\sigma}} \end{pmatrix} = E_n \begin{pmatrix} u^n_{\mathbf{i}\sigma} \\ v^n_{\mathbf{i}\bar{\sigma}} \end{pmatrix} , \quad (2)$$

where $\mathcal{H}_{\mathbf{ij}\sigma} = -t_{\mathbf{ij}} + (U\langle n_{\mathbf{i}\sigma}\rangle - \mu)\delta_{\mathbf{ij}}$. Here, we choose the nearest-neighbor hopping $\langle t_{\mathbf{ij}}\rangle = t = 1$ and the next-nearest-neighbor hopping $\langle t_{\mathbf{ij}}\rangle = t' = -0.25$ to match the curvature of the Fermi surface for most cuprate superconductors [10]. The exact diagonalization method to self-consistently solve BdG equations with the periodic boundary conditions is employed to get the N positive eigenvalues (E_n) with eigenvectors ($u^n_{\mathbf{i}\uparrow}, v^n_{\mathbf{i}\downarrow}$) and N negative eigenvalues ($\bar{E}_n$) with eigenvectors ($-v^{n*}_{\mathbf{i}\uparrow}, u^{n*}_{\mathbf{i}\downarrow}$). The self-consistent conditions are

$$\begin{aligned} \langle n_{\mathbf{i}\uparrow}\rangle &= \sum_{n=1}^{2N} |\mathbf{u}^n_{\mathbf{i}}|^2 f(E_n) , \ \langle n_{\mathbf{i}\downarrow}\rangle = \sum_{n=1}^{2N} |\mathbf{v}^n_{\mathbf{i}}|^2 [1 - f(E_n)] , \\ \Delta_{\mathbf{ij}} &= \sum_{n=1}^{2N} \frac{V}{4} (\mathbf{u}^n_{\mathbf{i}} \mathbf{v}^{n*}_{\mathbf{j}} + \mathbf{v}^{n*}_{\mathbf{i}} \mathbf{u}^n_{\mathbf{j}}) \tanh(\frac{\beta E_n}{2}) , \end{aligned} \quad (3)$$

where $\mathbf{u}^n_{\mathbf{i}} = (-v^{n*}_{\mathbf{i}\uparrow}, u^n_{\mathbf{i}\uparrow})$ and $\mathbf{v}^n_{\mathbf{i}} = (u^{n*}_{\mathbf{i}\downarrow}, v^n_{\mathbf{i}\downarrow})$ are the row vectors, and $f(E) = 1/(e^{\beta E} + 1)$ is Fermi-Dirac distribution function. Since the calculation is performed near the optimally doped regime, the filling factor, $n_f = \sum_{\mathbf{i}\sigma}\langle c^\dagger_{\mathbf{i}\sigma} c_{\mathbf{i}\sigma}\rangle / N_x N_y$, is fixed at 0.85, i.e., the hole doping $\delta = 0.15$. Each time when the on-site repulsion U or the temperature is varied, the chemical potential μ needs to be adjusted .

In Fig. 1(a), we use $U = 2.44$ and $V = 1.0$ to approximately reproduce the phase diagram of Inaba *et al.* [5] based on a mean field approach of the $t-J$ model, there the contribution from the AF order was explicitly considered. We shall apply this phase diagram to understand the experimental observations in Ref. [1]. It is important to notice that the curve (dashed line) separating the region of the dSC and the coexistence region of dSC plus SDW in the phase diagram has a positive slop as the doping (δ) increases. The detailed structure of the SDW in the underdoped region is not the main focus of the present paper and will not be presented here. From the phase diagram, if $\delta = 0.15$ is chosen near the optimal doping or in the slightly underdoped region, one can easily see that at low temperature T, our system is in the phase of dSC. When T increases, the SDW order emerges and coexists with the dSC. At very higher T, the dSC disappears and only SDW order survives. These temperature dependencies can be understood from Fig. 1(b) where the dSC order parameter at site $\mathbf{i}$ and the maximum value of the staggered magnetization $M_{\mathbf{i}}$ are plotted as functions of temperature T/t. From Fig. 1(b), it is straightforward to show that only dSC exists and the AF order is completely suppressed at low T. As $T > 0.06t$, the stripe-modulated AF or the SDW order incipit, and both of

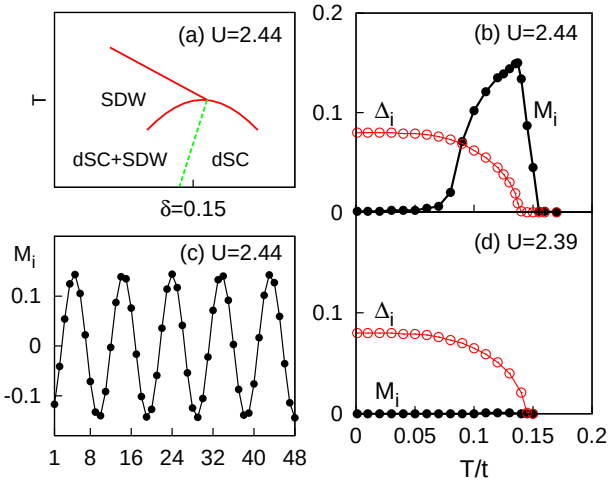

FIG. 1: (a) The phase diagram for $U = 2.44$. (c) The projection of the staggered magnetization $M_{\mathbf{i}}$ at $T = 0.84T_N$, where $M_{\mathbf{i}} = (-1)^{\mathbf{i}}(n_{\mathbf{i}\uparrow} - n_{\mathbf{i}\downarrow})$. The size of the unit cell is $N_x \times N_y = 48 \times 24$. (b) and (d) show the temperature dependence of the dSC (open circle) and the maximum value of $M_{\mathbf{i}}$ (solid circle) for $U = 2.44$ and $U = 2.39$, respectively. The value of the dSC order parameter $\Delta_{\mathbf{i}} = \frac{1}{4}(\Delta_{\mathbf{i}+\hat{x}} + \Delta_{\mathbf{i}-\hat{x}} - \Delta_{\mathbf{i}+\hat{y}} - \Delta_{\mathbf{i}-\hat{y}})$ is measured in the unit of t.

them could persist above the BCS transition temperature $T_c^{BCS} = 0.14t$. At $T > T_c^{BCS}$, the staggered magnetization decreases rapidly to zero at the Neel's temperature $T_N = 0.155t$. In Fig. 1(c) we show that the projection of the y-oriented stripe modulation in the AF order (or SDW) at $T = 0.84T_N < T_c^{BCS}$ along x-axis, where the SDW has mixed periodicity $10a - 9a - 10a - 9a - 10a$ over a $48a \times 24a$ lattice. The periodicity of the SDW seems not sensitive to T as long as the SDW order is in presence. In Fig. 1(d), we make similar plots as those in Fig. 1(b) but with a smaller $U = 2.39$. In this case the AF order is completely suppressed and our system is in the state of pure dSC at all temperatures. This implies that the phase diagram for $U = 2.39$ should be similar to that in Fig. 1(a) except the phase boundary (dashed line) is pushed toward the lower doped region. In both figures 1(b) and 1(d), the dSC order parameter as a function of T appears to have the BCS-like behavior. Besides, the T_c^{BCS} in the case for $U = 2.39$ [Fig. 1(d)] is slightly larger than the one for $U = 2.44$ [Fig. 1(b)]. This is because the appearance of SDW in Fig. 1(b) at higher T also suppresses the dSC. It needs to point out here that a phase diagram of the same model was previously studied by Martin *et al.* [7] using a very larger U on a much smaller lattice ($17a \times 10a$). The curve separating the region of dSC and that of dSC plus SDW in their phase diagram has a negative slop. And that would yield the conclusion that if the system is in pure dSC state at low temperature, then it is always in dSC state at a temperature up to $T < T_c^{BCS}$ and the SDW order never shows up. This is very different from the present

situation. In the following we show that the results in Figs. 1(b) and 1(c) can be applied to understand various features observed in the STM experiment [1].

At finite temperature, what the STM measures is the LDTC which has the following definition

$$G_{\mathbf{i}}(E)_T \equiv \left.\frac{dI_{\mathbf{i}}}{dE}\right|_T = A\int \rho_{\mathbf{i}}(E')_T\left[-\frac{d}{dE}f(E'-E)\right]dE' \quad (4)$$

, where

$$\rho_{\mathbf{i}}(E)_T = -\frac{1}{M_x M_y}\sum_{n,\mathbf{k}}^{2N}\left[\left|\mathbf{u}_{\mathbf{i}}^{n,\mathbf{k}}\right|^2 f'(E_{n,\mathbf{k}}-E) + \left|\mathbf{v}_{\mathbf{i}}^{n,\mathbf{k}}\right|^2 f'(E_{n,\mathbf{k}}+E)\right] \quad (5)$$

is the LDOS, and A is proportional to the square of the tunnelling matrix element. The summation in $\rho_{\mathbf{i}}(E)_T$ is averaged over $M_x \times M_y$ wavevectors in first Brillouin Zone.

In Fig. 2, the normalized LDOS (a) and LDTC (b) at the sites with the maximum staggered magnetization ($M_{\mathbf{i}}$) as functions of the bias energy E are presented from low to high temperatures. It is clear from Eq. (4) that the LDTC reduces to LDOS at low T. But at higher T, the behavior of the LDTC is rather different from that of the LDOS. For example, the characteristic temperature T_c^{bulk}, where the coherent peaks of the superconductivity begin to flatten out, in the LDTC is considerably lower than that in the LDOS. One usually define the gap of the quasiparticles as the separation between the coherent peaks or the width of the dip or depression in the LDOS. While the gap in the LDOS [Fig. 2(a)] appears roughly to be a constant from low T up to T_N, the "gap" in the LDTC [Fig. 2(b)] increases progressively from low T to high T. The increment in the magnitude of "gap" as T raises has been indeed observed by experimental measurements [11, 12, 13]. It should be emphasized here that the "gap" in the LDTC or observed directly from the STM experiments is the result of the convolution in Eq. (4) and may not be the real gap of the system. In the temperature range of $T_c^{bulk} < T < T_N$ as shown in Fig. 2, the system appears to be in the "pseudogap" region according to the characterization from STM experiments [9, 14]. Even though the effect due to the phase fluctuations on the dSC order parameter [15, 16] has not been taken into account. In this region, the Fermi surface in our theory is everywhere gaped while the ARPES experiment [17] indicates that the gaps occur only near $(\pm\pi, 0)$ and $(0, \pm\pi)$. This difficulty so far has not been understood.

It is well established that associated with the SDW shown in Fig. 1 (c), there are stripe-modulations in the dSC order and the charge density. The stripe modulated charge order can also be refereed to the charge density wave (CDW). In the top two graphs of the left panel in

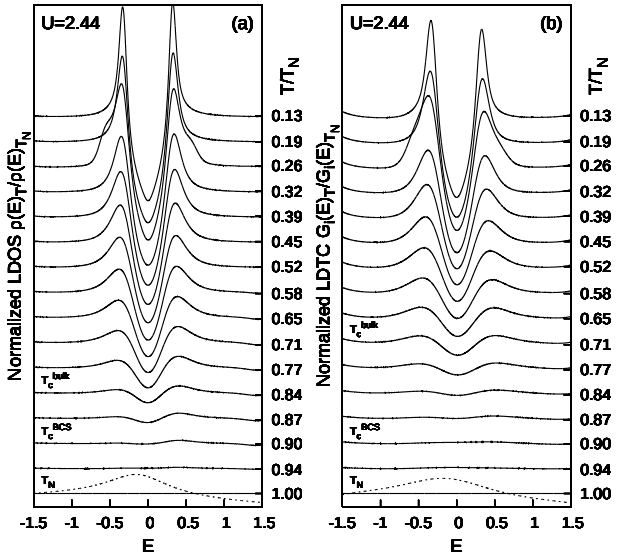

FIG. 2: Temperature dependence of the normalized LDOS ($\rho_{\mathbf{i}}(E)_T/\rho_{\mathbf{i}}(E)_{T_N}$) and the normalized LDTC ($G_{\mathbf{i}}(E)_T/G_{\mathbf{i}}(E)_{T_N}$), here $T_N = 0.155t$. The LDOS and LDTC at T_N as a function of E is represented by the dashed line. This representative set of spectra was shifted vertically for clarity. The wavevectors in first Brillouin Zone are $M_x \times M_y = 24 \times 12$.

Fig. 3, the projections of the y-oriented stripe modulations in the dSC order and the charge density are plotted along the x-axis at $T = 0.84T_N(< T_c^{BCS})$. Here the spatial distributions of the dSC and the charge order are only slightly modulated by the stripe structure, and the dSC and the SDW orders coexist in real space. This feature is very different from the case in Ref. [7], where the dSC order is practically suppressed to zero in the spatial regions where the AF order is in presence. The stripe modulation also appears in the LDTC (or LDOS) as shown in the bottom graph of the left panel. The stripe modulations displaced in the left panel have the same mixed periodicity $5a - 5a - 4a - 5a - 5a$ over a $24a$ lattice along x-axis. This indicates that the system is trying to establish a periodicity incommensurate with the underline lattice, but fails to do so because the calculation is performed in a discrete and finite lattice, not in a continuum. It is also straightforward to show that the same mixed periodicity still remains in the CDW and LDTC (or LDOS) even T is in the region of $T_c^{BCS} < T < T_N$, where the superconducting order parameter vanishes and the SDW order is still in presence. As it will be shown below that an average periodicity $4.8a$ for the stripe modulation could be assigned in the present case. The x- and y- oriented stripe modulations are degenerate in energy, and it is thus possible for the both x- and y- oriented stripe-modulations to show up either in the time duration when the experiment is performed or due to the proximity effect [8] between neighboring domains with stripes of

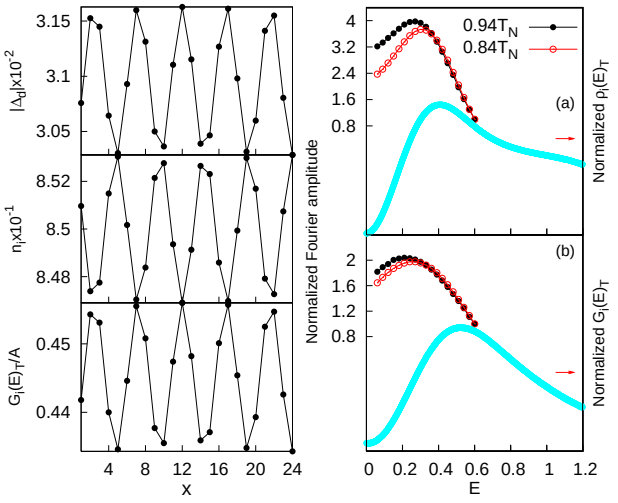

FIG. 3: Left panel: From top to bottom, the projection of the dSC order, charge density, and LDTC at $T = 0.84T_N$. Right panel: The energy evolution of the normalized Fourier amplitude of the LDOS (a) and LDTC (b) images for $T = 0.94T_N$ (solid circle) and $T = 0.86T_N$ (open circle) at $q_x = 0.417(\pi/a)$. The solid curve represents the normalized LDOS (a) and LDTC (b) as a function of E at $T = 0.84T_N$. The wavevectors which have been used to calculate the LDOS and LDTC images are $M_x \times M_y = 6 \times 6$ in first Brillouin Zone.

different orientations. As a result, checkerboard pattern could be observed.

Furthermore, in order to get a detailed understanding of the periodicity of the modulation in the LDOS (or LDTC) image, we perform the Fourier transform of the LDOS (or LDTC) image in the temperature range where the SDW order is in existence.

$$\rho_{\mathbf{q}}(E)_T = \frac{1}{\sqrt{N_x N_y}} \sum_{\mathbf{i}} exp(i\ \mathbf{q}\cdot\mathbf{r_i})\cdot\rho_{\mathbf{i}}(E)_T\ . \quad (6)$$

When the above quantity is plotted against q_x, a sharp peak occurs around $q_x = 0.417(\pi/a) = 2\pi/4.8a$, indicating an average "periodicity" $4.8a$ in real space. In Fig. 3(a) and 3(b), the solid curves at the bottom represent, respectively, the normalized LDOS and the normalized LDTC as functions of the bias energy at $T = 0.84T_N$. The curves at the top made of solid/open circles show the bias energy dependencies of the Fourier amplitudes of the LDOS and LDTC images at $q_x = 2\pi/4.8a$ for two different temperatures normalized by their values at $E = 0.6t$. The Fourier amplitude of the LDOS first reaches a peak and then drops somewhat rapidly as the bias decreases to zero. Near the zero bias, the result at $T = 0.84T_N (< T_c^{BCS})$ dips more than the result at $T = 0.94T_N (> T_c^{BCS})$ in the pseudogap region. On the other hand, the Fourier amplitude of the LDTC as functions of the bias energy at these two temperatures differ very little, and they drops only slightly after reaching a broader maximum from higher bias. This feature in the LDTC seems to be in better agreement with the STM measurements [1] as compared with that of the LDOS.

In conclusion, the temperature dependencies of the LDTC and LDOS in a cuprate superconductor with the competing AF order have been investigated in the present paper. According to our calculations based on the phase diagram in Fig. 1(a) near the optimal doping, there is no signature of the charge order in the LDOS and the LDTC at low T. When the SDW order appears, both of the LDOS and the LDTC exhibit the same CDW like modulation with an average periodicity $4.8a$ at T below and above T_c^{BCS}. We also calculate the Fourier amplitude of LDOS and LDTC at $\mathbf{q} = (2\pi/4.8a, 0)$ and their bias energy dependencies in the "pseudogap" region as shown in Figs. 3(a) and 3(b), respectively. All the features in the LDTC are in good agreement with those observed by the STM experiments [1]. Finally we point out that the "gap" of the quasiparticles at higher T obtained directly from the LDTC or the STM experiments does not correspond to the real gap of the system in cuprate superconductors.

Acknowledgements: We thank S.H. Pan, J.X. Zhu and Q. Yuan for useful comments and suggestions. This work is supported by the Texas Center for Superconductivity and Advanced Material at the University of Houston, and by a grant from the Robert A. Welch Foundation.

[1] M. Vershinin, S. Misra, S. Ono, Y. Abe, Y. Ando, and A. Yazdani, Science **303**, 1995 (2004).
[2] J.E. Hoffman, K. McElroy, D.-H. Lee, K.M. Lang, H. Eisaki, S. Uchida, and J.C. Davis, Science **297**, 1148 (2002).
[3] K. McElroy, R.W. Simmonds, J.E. Hoffman, D.-H. Lee, J. Orenstein, H. Eisaki, S. Uchida, and J.C. Davis, Nature **422**, 520 (2003).
[4] T. Giamarchi and C. Lhuillier, Phys. Rev. B **43**, 12943 (1991).
[5] M. Inaba, H. Matsukawa, M. Saitoh, and H. Fukuyama, Physica C **257**, 299 (1996).
[6] M. Inui, S. Doniach, P. J. Hirschfeld, and A. E. Ruckenstein, Phys. Rev. B **37**, R2320 (1988).
[7] I. Martin, G. Ortiz, A.V. Balatsky, and A.R. Bishop, Europhys. Lett., v. **56**, 849 (2001)
[8] C. Howald, H. Eisaki, N. Kaneko, M. Greven, and A. Kapitulnik, Phys. Rev. B **67**, 014533 (2003).
[9] M. Kugler, Ø. Fischer, Ch. Renner, S. Ono, and Y. Ando, Phys. Rev. Lett. **86**, 4911 (2001).
[10] M.R. Norman, Phys. Rev. B **63**, 092509 (2001).
[11] T. Timusk and B. Statt, Rep. Prog. Phys. **62**, 61 (1999).
[12] Y. Xuan, H.J. Tao, Z.Z. Li, C.T. Lin, Y.M. Ni, B.R. Zhao, and Z.X. Zhao, cond-mat/0107540.
[13] S.H. Pan, Private communication.
[14] Ch. Renner, B. Revaz, J.-Y. Genoud, K. Kadowaki, and Ø. Fischer, Phys. Rev. Lett. **80**, 149 (1998).
[15] V. Emery and S. Kivelson, Nature **374**, 434 (1995).
[16] M. Franz and A.J. Millis, Phys. Rev. B **58**, 14572 (1998).

[17] M. R. Norman, H. Ding, M. Randeria, J.C. Campuzano, T. Yokoya, T. Takeuchi, T. Takahashi, T. Mochiku, M. kadowaki, P. Guptasarma, and D.G. Hinks, Nature **392**, 157 (1998).